Microstructure and Texture of Polycrystalline CVD-ZnS Analyzed via EBSD

Tilman Zscheckel, Wolfgang Wisniewski, and Christian Rüssel*

Polycrystalline ZnS samples are studied using X-ray diffraction and scanning electron microscopy including electron backscatter diffraction (EBSD). The material is industrially produced by a chemical vapor deposition process (CVD). Near the substrate, crystal growth leads to grains smaller than 50 μm in the cut plane. Elongated crystals with visible lengths of up to 400 μm are formed further from the substrate. These crystals are heavily twinned and exhibit Σ3 grain boundaries (i.e., the orientation of one {111}-plane is constant while rotations of 60° around its normal occur). About 1000 μm from the substrate, the grain size shrinks to about 20 μm along an abrupt border; a continuous grain size transition is not observed. Gradual orientation changes within single grains occur and in some cases lead to the fragmentation of grains parallel to the direction of growth. This is preferably observed in smaller grains more than 1000 μm from the substrate. Twinning, on the other hand, predominantly occurs in the large grains near the substrate. Both mechanisms should contribute to stress minimization in the sample. Textures of the analyzed surfaced indicate a general <001>-orientation perpendicular to the substrate and thus parallel to the direction of crystal growth.

1. Introduction

Polycrystalline zinc sulfide (ZnS) is a favorable material for applications where transparency for light in a wide range of wave lengths is required as it is principally transparent from 340 nm to 10.5 μm.[1,2] In commercial optical devices incorporating polycrystalline zinc sulfide a transmission of > 74% is usually not obtained at wavelengths below 420 nm[1,2] due to increased light scattering at smaller wavelengths. Polycrystalline ZnS is produced in an industrial scale via a CVD process[2,3] where the reactor is flushed with H_2S-gas of well defined partial pressure while metallic zinc is heated above its melting point (420 °C) to produce Zn-vapor. The walls of the reaction chamber are made of graphite where ZnS is deposited after the reaction:

$$\mathrm{Zn(g) + H_2S\,(g) \rightarrow ZnS\,(s) + H_2\,(g)}\,, \quad (1)$$

during which gaseous hydrogen is formed simultaneously. Trace quantities of hydrogen are incorporated in the deposited ZnS layer and lead to a characteristic absorption at a wavelength of 6 μm due to Zn-H vibrations.[2]

T. Zscheckel, Dr. W. Wisniewski, C. Rüssel
Otto-Schott-Institut
Fraunhoferstr. 6, 07743, Germany
E-mail: wolfgang.w@uni-jena.de

DOI: 10.1002/adfm.201103131

Two equally dense phases (4.09 g/cm^3) of ZnS occur: cubic zincblende (β -ZnS) and hexagonal wurtzite (α-ZnS). The dominantly occurring zincblende[2] is thermodynamically stable at temperatures up to 1023 °C[4] and shows a cubic face centered symmetry of the space group $F\bar{4}3m$ with a = 5.406 Å (JCPDS 00-005-0566). Wurtzite is thermodynamically stable above 1023 °C. $P6_3mc$ is the space group of wurtzite with the lattice parameters of a = 3.8227 Å and c = 6.2607 Å (JCPDS 01-179-2204). Various polytypes of ZnS have also been described.[5] The sublimation point of ZnS is 1185 °C.[4] A tendency to form elongated grains, lamellae and twins during crystal growth is reported in the literature.[3] Furthermore, a texture has been reported where one crystallographic direction of the <001>-family is oriented perpendicular to the substrate layer.[2,3,6] Currently ZnS is produced using the above mentioned CVD process followed by subsequent hot isostatic pressing which eliminates the Zn-H-vibration band at 6 μm and increases the optical transmission at wavelengths in the visible range.

The main part of the experimental work presented here has been performed using electron backscatter diffraction (EBSD). This method is carried out in a scanning electron microscope (SEM) and enables to quantitatively describe the crystal phase formed in each point of the micrograph with a minimum resolution of about 10 nm. Furthermore, the orientation of the crystals in each point is determined.[7–9] In the past few years this method gained in interest also with respect to the quantitative description of oriented polycrystalline materials.[7–9]

In this paper, the structure, texture and twinning of polycrystalline CVD-ZnS are characterized using SEM and EBSD as well as X-ray diffraction (XRD) to gain further insight into the crystal growth mechanisms occurring during the CVD process.

2. Results and Discussion

After removal from the reactor, polycrystalline CVD-ZnS is opaque and yellow. If the graphite of the substrate is removed by etching, the surface is very rough and only individual EBSD-patterns can be obtained from the first deposition layer, making scans impossible. The opposite side, i.e. the growth front as presented in **Figure 1**a is rough and covered by spherical mounds. Contact between the mounds leads to deviations from

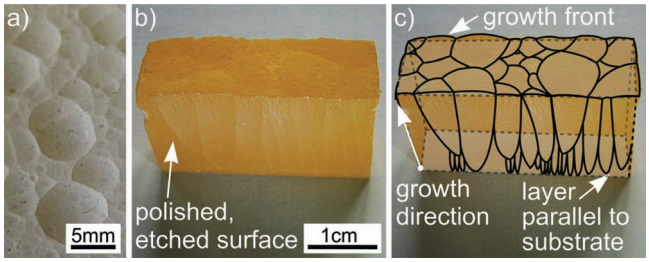

Figure 1. a) CVD-ZnS growth front after the process. b) CVD-ZnS polished and etched, illuminated with an angular light incidence. c) Outlines of the growth structures.

the spherical geometry. Figure 1b shows an etched sample cut perpendicular to the substrate layer and thus parallel to the growth direction. Under an angular light incidence macroscopic, cone-like structures are seen. The boundaries between the etched structures are visualized in Figure 1c. The cones are densely packed and show increasing diameters with the distance from the substrate. The mounds at the growth front can be correlated to the cones. While a slight brightness gradient is observed inside individual cones (see Figure 1b), a high contrast is observed between neighboring cones. Hence these cones must be micro-polycrystalline as single crystals would show homogeneous light reflection across their entire surface.

Figure 2 shows XRD-patterns of various CVD-ZnS samples cut perpendicular to the growth direction as well as the theoretical patterns of a) wurtzite and b) zincblende. Figure 2c was recorded from a sample representing the first layer at the substrate. Figure 2e presents data from a cut plane 1 mm below this first layer and Figure 2g was recorded from the growth front, i.e. at a distance of approximately 13 mm from the first layer. The patterns d) and f) are more detailed versions of the patterns c) and e) to visualize the peaks of minor intensity barely discernible in the later patterns. Zincblende is the main phase in all XRD-patterns. Other phases are not detected except in the pattern shown in Figure 2d where minor concentrations of wurtzite are also observed. While the intensities of the XRD-peaks observed in the first deposition layer match a statistic orientation distribution for zincblende, hints of orientational changes are observed as crystal growth proceeds. Comparing the patterns Figure 2c,e and g shows that the relative intensities of the peaks change with the distance from the growth front. While a statistical distribution is observed at the substrate, the {002}-peak is increasingly exaggerated as growth proceeds. This is in agreement to the literature[2,3,6] and indicates that an orientation selection occurs during crystallization, leading to a texture in which the <001>-direction is perpendicular to the substrate and thus parallel to the growth direction.

The SEM micrograph presented in **Figure 3** was recorded directly from the growth front of the CVD-ZnS. The growth front has a notable topography and is not at all smooth. It should be noted that the structure seen in Figure 3 is much smaller than the spherical mounds shown in Figure 1a. The inset in Figure 3 shows a micrograph with a higher magnification where a sub-structure is observed; this lamellar structure is probably caused by the growth process.

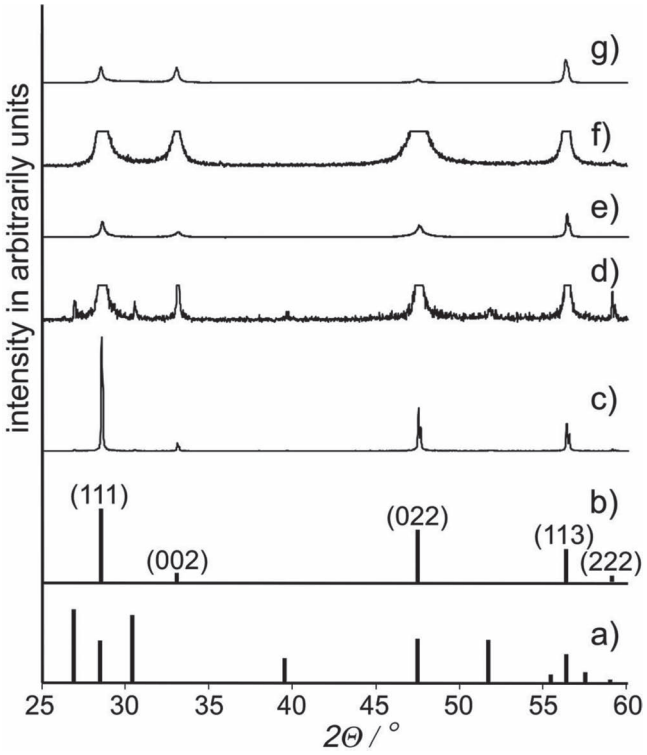

Figure 2. XRD-patterns of CVD-ZnS: theoretical intensities of a) wurtzite (JCPDS 01-079-2204) and b) zincblende (JCPDS 00-005-0566). Pattern c) describes the growth approach, pattern d) is a more detailed version of the same pattern visualizing peaks of lower intensity. Pattern e) describes the material about 1 mm from the substrate, while pattern f) is a more detailed version of the same pattern. Pattern g) was obtained from the growth front also presented in Figure 1a.

High quality Kikuchi patterns were obtained from polished surfaces and could be reliably indexed as cubic ZnS while no pattern could be indexed as wurtzite with absolute certainty. **Figure 4** shows the SEM-micrograph of a polished cut plane superimposed by the combined Inverse Pole Figure and Image Quality-map (IPF+IQ-map) showing the orientation of every

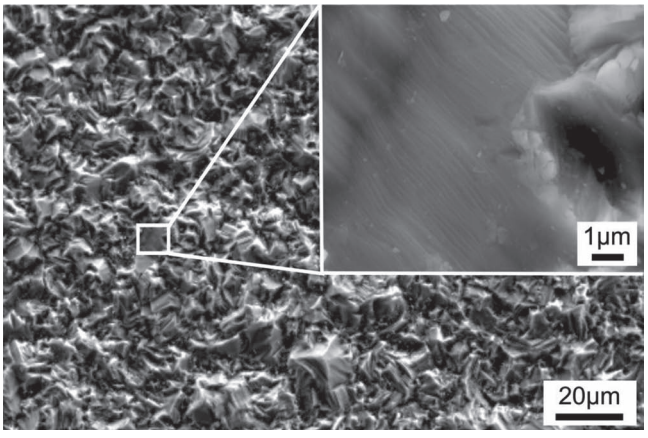

Figure 3. SEM micrograph of the growth front of CVD-ZnS also presented in Figure 1a.

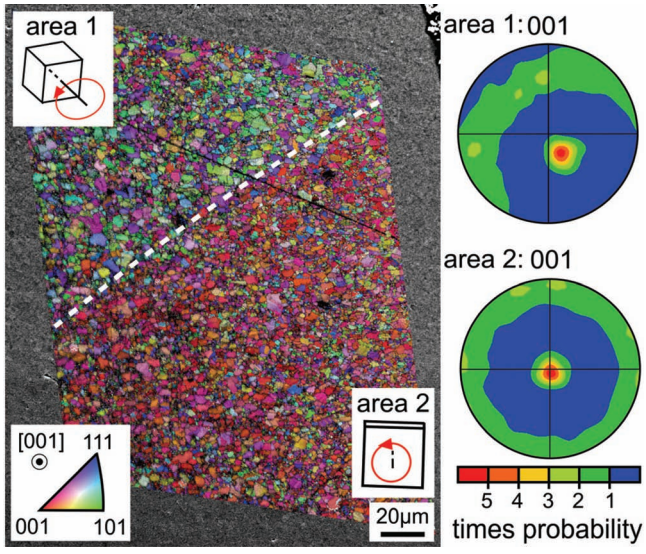

Figure 4. SEM micrograph of a sample cut perpendicular to the growth direction superimposed by the combined IPF+IQ-map of an EBSD scan. The pole figures describe the <001>-textures observed in areas 1 and 2. Unit cells illustrate the preferred orientation while the red arrows indicate free rotation around the <001>-direction.

point of the image. Discrete grains are discernable by a homogeneous color as well as the surrounding grain boundaries which appear darker due to lower IQ-values. The dashed white line separates two differently oriented regions of equal texture as green dominates the upper region (area 1), while the lower region (area 2) is predominantly red.

The 001-pole figures of textures calculated from these areas are also presented in Figure 4. Both pole figures indicate that the <001>-direction is preferably oriented perpendicular to the current surface and hence parallel to the main direction of crystal growth. The <001>-direction of area 1 deviates from that of area 2 by about 28°. The observed ring is caused by the poles of the other {001}-planes in the cubic system and indicates that the rotation around the <001>-direction is statistical. This is illustrated by the red arrows in the unit cells. The degree of orientational preference within the areas is comparable. The dominant orientation as well as the free rotation around a <001>-crystal direction is illustrated by the respective unit cells in Figure 4. These two regions represent two of the cone-like structures presented in Figure 1. Hence the cone-like structures in Figure 1 are not regions of homogeneous crystal orientation but rather textured polycrystalline structures.

Figure 5 shows the combined IPF+IQ-map of a sample cut parallel to the growth direction. The scan covers the first 1700 µm of deposited ZnS (the sample grew from the right to the left). Pores in the material appear black. In zone 1, the grains are only a few micrometers long near the substrate. The 001-pole figure indicates an almost statistical orientation distribution.

In zone 2, the grains increase in size as growth proceeds until they are notably elongated and some hundred µm in length. These grains contain lamellae which generally show two different orientations within a grain.

The formation of large grains stops at a distance of about 1000 µm from the substrate. During the following 100 µm of

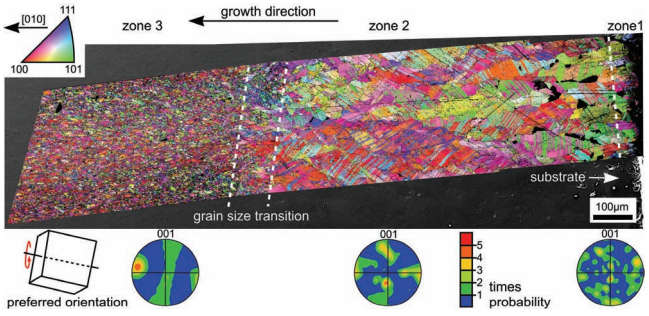

Figure 5. SEM micrograph of a sample cut parallel to the growth direction showing the first 1700 µm of the deposited material. The superimposed IPF+IQ-map of an EBSD-scan describes the orientations with respect to the [010]-direction indicated in the IPF-legend. Pole figures of textures calculated from the zones 1–3 describe the preferred orientations in the respective zones of crystallization.

material deposition the grain length is reduced to less than 25 µm without the occurrence of intermediate grain sizes, i.e. continuous changes are not observed. These smaller grains in zone 3 are also elongated in the growth direction and predominantly show orientations corresponding to red colors in the IPF. The corresponding 001-pole figure clearly shows the preferred orientation with a <001>-crystal direction parallel to the growth direction, ratifying the impression gained from the map, and indicates a statistical rotation around the <001>-direction by the band in the middle of the pole figure.

Considering the grain size in Figure 5 and the location of the corresponding cut plane with respect to the substrate, it can be concluded that the data in Figure 4 also describes the crystallization of zone 3 in Figure 5. The pole figures also match when considering the respective cut planes.

Figure 6a shows homogeneously oriented lamellae in a large grain from zone 2 in Figure 5. The Kikuchi bands evaluated in

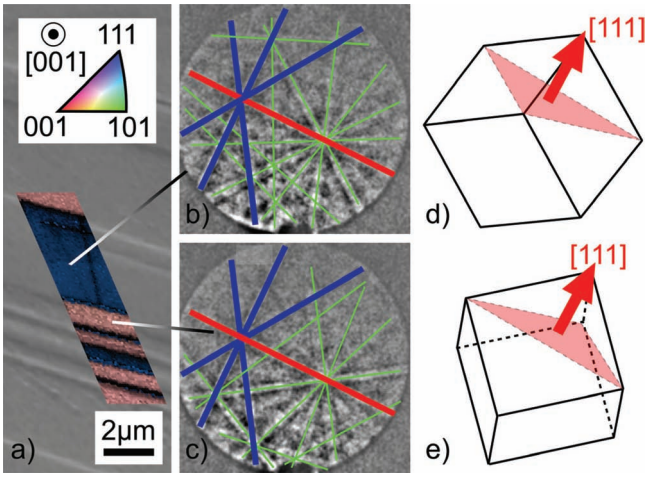

Figure 6. SEM micrographs: a) lamellae in a grain from zone 2 in Figure 5 superimposed by the IPF+IQ-map of an EBSD scan. The lines point to the EBSD patterns (b) and (c), obtained from the respective areas and superimposed by lines illustrating commonalities (red, blue) and differences (green) in the patterns. d,e) The unit cells describe the respective orientations and the position of the shared {111}-plane.

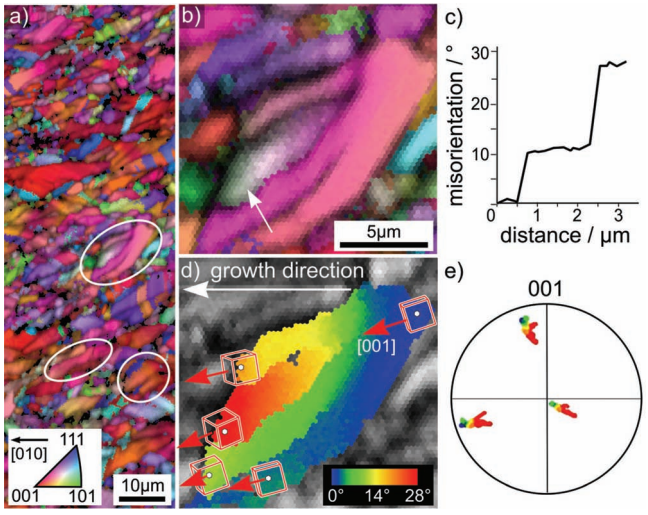

Figure 7. a) SEM micrograph of a sample cut perpendicular to the growth direction and superimposed by the IPF+IQ-map of an EBSD-scan. The reference system is outlined by the [010]-direction in the IPF legend. The ellipses mark crystals that changed their orientation during growth. b) Magnified part of the IPF+IQ-map containing a fragmenting grain. c) Misorientation profile along the arrow in Figure 7b. d) Orientation+IQ-map of the fragmenting grain superimposed by unit cells illustrating orientations. e) Pole figure of the fragmenting grain illustrating the spread of crystal orientations.

the respective patterns b) and c) are presented as well as the corresponding unit cells d) and e). The Kikuchi band attributed to the {111}-plane is drawn in red. This line, as well as the Kikuchi bands drawn in blue, occur in both patterns and are caused by equivalent lattice planes. Differing bands are drawn in green. Both patterns are attributed to two orientations of zincblende. The angle between both orientations is 60° and they share a parallel {111}-plane, as illustrated in the unit cells. Thus the lamellae share a common {111}-rotation plane, indicating the boundaries between the matrix and the lamellae are Σ3 twin boundaries.[10,11]

Figure 7a presents the combined IPF+IQ-map of a sample cut parallel to the growth direction covering material about 18 mm from the substrate. The small grain size indicates the crystal growth here is comparable to that of zone 3 in Figure 5. Some of the observed grains are twinned, illustrating that this mechanism also occurs in crystals more than 1000 µm from the substrate.

Some grains in the scan change their orientation as growth proceeds and are marked with white ellipsis. This effect is most pronounced in the grain featured in Figure 7b) in greater detail. Figure 7c) presents the point to origin misorientation along the arrow in Figure 7b and shows two steps of about 10° and 17° with only a minimal change between them. The combined orientation+IQ-map of the grain is presented in Figure 7d superimposed by selected unit cells in which one <001>-direction is indicated by a red arrow. Figure 7e shows the corresponding 001-pole figure illustrating the orientational change in the grain where blue is the common point of origin.

The initially homogeneous grain (upper right corner) is split into four parts which deviate from the initial orientation at different rates and extents. While the lowest branch only shows a maximum orientation deviation of about 4° over a distance of 16 µm, i.e. changes with 0.25°/µm, the second branch from the top (red) deviates from the initial orientation by up to 28° over only 14 µm, i.e. an average change in the orientation of 2.00°/µm. Within the segments, the orientation never changes more than 1° between two measured points at a stepsize of 0.25 µm. By contrast, the deviation between points in different segments along the arrow in Figure 7b is up to 17°, i.e. in a similar range as classic grain boundaries.

During the production of ZnS via the CVD process, fairly large, elongated, heavily twinned crystals with lengths of some hundred µm are formed within the first 1000 µm of crystal growth; they also contain some pores. The XRD-patterns indicate small quantities of hexagonal wurtzite near the substrate. EBSD-analysis of the initial growth layer directly at the substrate is very problematic as the patterns are of insufficient quality and scans are not possible without polishing, which would, however, remove the area of interest. While the hexagonal phase could not be identified with certainty via EBSD, it was possible to index the patterns as the cubic phase. The identified grains are preferably oriented with the <001>-direction approximately parallel to the growth direction. The twin boundaries are of the Σ3 type; the reason for their formation should be the minimization of stresses formed during the growth process. Wurtzite is the hexagonal high temperature modification of ZnS[4] and hence the energy of the stacking faults is negative at room temperature.[12] This means wurtzite may continuously transfer to zincblende and the splitting of dislocations accompanied by the introduction of stacking faults is energetically advantageous.[10–12]

It should be noted that the observed texture cannot be the result of epitaxial growth of cubic ZnS on the substrate, because the substrate is composed of untextured polycrystalline graphite. Instead the orientation is achieved by the growth mechanism, i.e. by different crystal growth velocities in different crystallographic directions. The Van der Drift Model of competitive crystal growth in CVD layers predicts a texture under the assumption of infinite surface diffusion.[13] Here crystals which grow fastest perpendicular to the substrate survive, while crystals of other orientations hinder each other during crystal growth. The degree of orientation increases with the film thickness.[13,14] In the results presented here, the <001>-crystal direction is perpendicular to the substrate, but a perfect orientation is never achieved. Instead, the degree of crystal orientation remains nearly constant after the change in grain size at 1000 µm.

Oriented crystallization not based on an epitaxial mechanism has been reported for processes such as the dewetting of gold layers on amorphous substrates such as oxidized wafers[15] and also for glass crystallization.[16,17] The latter is accompanied by the formation of oriented nuclei at the surface.[16,17]

After about 1000 µm of crystal growth, the grain size decreases significantly. Twinning is still observed but additionally twisted grains are formed. Some crystals show a continuous change of the orientation over the length of the crystal, the maximum rate of orientational change observed within one crystal was 2°/µm. In contrast to the formation of twin boundaries, the orientational changes within one grain are continuous

and do not take discrete values. The reason for these twisted grains should also be the minimization of stresses. It should be noted that the first few millimeters of ZnS are removed for the preparation of optical devices from CVD-ZnS, i.e. the coarse, elongated, heavily twinned grains are not utilized for industrial applications. The reason for the formation of small ZnS grains after about 1000 μm crystal growth is still unclear. It seems plausible that thermal reasons, especially a decrease in temperature at the growth front might play an important part due to decreasing thermal conduction caused by the growing CVD layer.

Indications for the formation of a texture in the ZnS-layer during the CVD process have been given via XRD-measurements[2,3,6] in agreement with those presented in Figure 2. A quantitative description of the development during crystal growth, however, was not presented. Additionally, stacking faults in the cubic lattice have been reported in the literature.[18] The observation that some XRD-peaks were shifted to smaller 2θ-values while others were shifted to larger values was interpreted as the effect of stacking faults. It should be noted that a very high density of stacking faults is necessary to notably affect the XRD-patterns. In the material studied in this paper, the density of twin boundaries are of the Σ3 type is not high enough to notably affect XRD-patterns.

The most frequently studied cubic system comparable to CVD-ZnS is the diamond system. Although, diamond is not thermodynamically stable at standard pressure, the formation of diamond using CVD processes is possible as first reported in 1952.[19] In analogy to ZnS, CVD-diamond can also be textured.[20] If the diamond crystals are oriented with the <001>-direction perpendicular to the substrate, the crystals are relatively free of planar defects.[21] If, however, crystals are oriented with the <111>-direction perpendicular to the substrate, heavy primary twinning parallel to the oriented {111}-plane of the diamond lattice is observed.[22] CVD diamond grown on molybdenum has already been the subject of EBSD studies[20] and led to results comparable to those presented for CVD-ZnS here. It can be concluded that some similarities regarding the structure of ZnS and diamond exist if both are formed by a CVD process.

3. Conclusions

Industrially produced polycrystalline ZnS samples prepared by a CVD process were studied using XRD and SEM including EBSD. At the beginning of the growth process, fairly small crystals were formed. After a few micrometers, elongated grains with sizes of some hundred micrometers are formed. About 1000 μm from the substrate the grain size is abruptly reduced to lengths smaller than 50 μm.

The large, elongated crystals are heavily twinned and show a high density of Σ3 twin boundaries. The smaller grains formed after the grain size transition at 1000 μm are also twinned. Some grains show a change in their orientation during crystal growth up to 2°/μm. Nevertheless, a <001>-direction is preferentially oriented parallel to the growth direction. Twinning occurs by rotations of 60° around the normal of one {111}-plane of the individual grains.

4. Experimental Section

Industrially produced samples of polycrystalline ZnS were studied. The ZnS layers with a thickness of around 30 mm were synthesized by chemical vapour deposition (CVD) from zinc vapour and H_2S on a graphite substrate. The samples were provided by Vitron GmbH (Jena, Germany).

Samples of various sections parallel or perpendicular to the substrate were polished using decreasing grain sizes of diamond paste. Some of the samples were embedded in polymer before polishing. Macroscopic structure effects were visualized by etching polished samples with potassium ferricyanide ($K_3Fe(CN)_6$).

To achieve a surface quality appropriate for EBSD-analysis a final finish of colloidal silica was applied. Surface charging in the SEM was avoided by contacting the samples with Ag-paste and applying a thin layer of carbon at about 10^{-3} Pa.

The samples were studied by X-ray diffraction (XRD) using a SIEMENS *D5000* diffractometer and CuKα radiation. SEM- and EBSD-analyses were performed using a scanning electron microscope Jeol JSM-7001F equipped with a TSL Digiview 1913 EBSD-camera. EBSD-scans were captured and evaluated using the programs TSL OIM Data Collection 5.31 and TSL OIM Analysis 5. The EBSD-scans were performed using a voltage of 20 kV. Only points with a minimum Confidence Index (CI) of 0.1 were considered in evaluations indicating the attributed orientation solutions are correct with a probability of at least 96%.[23]

Acknowledgements

This work was funded by the BMWI (ZIM program KF2519702FK1).

Received: December 24, 2011
Published online: July 25, 2012

[1] *Data Sheet: Technical Zincsulfide, Vitron Spezialwerkstoffe GmbH*, Jena, Germany **2008**.
[2] J. McCloy, R. Korenstein, *J. Am. Ceram. Soc.* **2009**, *92*, 1725.
[3] A. F. Shchurov, V. A. Perevoshchikov, T. A. Gracheva, N. D. Malygin, D. N. Shevarenkov, E. M. Gavrishchuk, V. B. Ikonnikov, E. V. Yashina, *Inorg. Mater.* **2004**, *40*, 96.
[4] O. Knacke, O. Kubaschewski, K. Hesselmann, in *Thermodynamical Properties of Inorganic Substances*, Springer, Berlin, Heidelberg, New York **1991**.
[5] V. Medizadeh, S. Mardix, *Acta Cryst.* **1986**, *C42*, 518.
[6] P. Biswas, R. S. Kumar, P. Ramavath, V. Mahendar, G. V. N. Rao, U. S. Hareesh, R. Johnson, *J. Alloys Compd.* **2010**, *496*, 273.
[7] J. A. Venables, C. J. Harland, *Philos. Mag.* **1973**, *27*, 1193.
[8] T. C. Isabell, V. P. Dravid, *Ultramicroscopy* **1997**, *67*, 59.
[9] S. Zaefferer, *Ultramicroscopy* **2007**, *107*, 254.
[10] G. Hasson, M. Biscondi, P. Lagarde, J. Levy, C. Goux, in *The Nature and Behaviour of Grain Boundaries*, (Ed: H. Hu), *The Metallurgical Society of AIME Proceedings*, Plenum Press, New York - London **1972**.
[11] V. Novikov *Grain Growth and Control of Microstructure and Texture in Polycrystalline Materials*, CRC Press, Boca Raton, FL **1997**.
[12] H. Blank, P. Delavicnett, S. Amelinckx, *Phys. Status Solidi* **1962**, *2*,1660.
[13] A. van der Drift, *Philips Res. Rep.* **1967**, *22*, 267.
[14] D. Meakin, J. Stoemenos, D. Miglierate, N. Economen, *J. Appl. Phys.* **1987**, *61*, 5031.
[15] M. Bechelany, X. Maeder, J. Riesterer, J. Hankache, D. Lerose, S. Christiansen, J. I. Michler, L. Philippe, *Cryst. Growth Des.* **2010**, *10*, 587.
[16] W. Wisniewski, T. Zscheckel, G. Völksch, C. Rüssel, *CrystEngComm* **2010**, *12*, 3105.

[17] W. Wisniewski, M. Nagel, G. Völksch, C. Rüssel, *Cryst. Growth Des.* **2010**, *10*, 1414.
[18] E. V. Karaksina, T. A. Gracheva, D. N. Shevarenkov, *Inorg. Mater.* **2010**, *46*, 6.
[19] R. S. Balmer, J. R. Brandon, S. L. Clewes, H. K. Dhillon, J. M. Dodson, I. Friel, P. N. Inglis, T. D. Madgwick, M. L. Markham, T. P. Mollart, N. Perkins, G. A. Scarsbrook, D. J. Twitchen, A. J. Whitehead, J. J. Wilman, S. M. Woollard, *J. Phys.: Condens. Matter* **2009**, *21*, 364221.
[20] T. Liu, D. Raabe, W. Mao, S. Zaefferer, *Adv. Funct. Mater.* **2009**, *19*, 3880.
[21] R. Clausing, L. Heatherly, L. Horton, E. Specht, G. Begun, Z. Wang, *Diamond Relat. Mater.* **1992**, *1*, 411.
[22] E. D. Specht, R. E. Clausing, L. Heatherly, *J. Cryst. Growth* **1991**, *114*, 38.
[23] D. P. Field, *Ultramicroscopy* **1997**, *67*, 1.